Far-field behaviours of steady capillary-gravity ship waves

Hui Liang & Xiaobo Chen
Deepwater Technology Research Centre (DTRC), Bureau Veritas, 117674, Singapore.
E-mail: hui.liang@sg.bureauveritas.com, xiao-bo.chen@bureauveritas.com

1. INTRODUCTION

An asymptotic analysis of capillary-gravity ship waves associated with a point perturbation is performed via establishing the relationship between dispersion curves on the Fourier plane and the corresponding wave pattern on the free surface. By using this relationship, far-field waves, ray-angles and phase & group velocities are determined in an explicit and simple way. Besides the speed threshold $c_{\min} \approx 0.2313$ m/s below which waves cannot be generated, another critical speed $c_{\text{fan}} \approx 0.4484$ m/s associated with the constitution of wave systems is obtained through studying inflection points along the dispersion curve. Behaviours of wave pattern and ray-angles for different velocities across the critical speed c_{fan} are investigated. Finally, a 2-point wavemaker model is adopted to investigate the interference between bow and stern waves.

2. STATEMENT OF THE PROBLEM AND DISPERSION RELATION

A 3D coordinate system $OXYZ$ steadily travelling with the ship at a speed c is defined with the XY plane coinciding with the undisturbed free surface and the OZ axis orienting positively upwards. Here, the reference length L and the gravitational acceleration g are used to define nondimensional coordinates (x, y, z), Fourier variables (α, β, k) and velocity potential ϕ as:

$$(x, y, z) = \frac{1}{F^2 L}(X, Y, Z), \quad \left(\alpha, \beta, k = \sqrt{\alpha^2 + \beta^2}\right) = F^2 L (A, B, K), \quad \phi = \frac{\Phi}{F^2 \sqrt{gL^3}} \tag{1}$$

where F denotes the Froude number defined as $F = c/\sqrt{gL}$. The characteristic wavenumber of capillary waves is $K_T = \sqrt{\rho g/T}$ [4] while the one for pure-gravity ship waves is $K_G = g/c^2$, so that the parameter σ associated with the surface tension effect is the ratio of both [2]:

$$\sigma = K_G/K_T = \sqrt{T/(\rho g L^2)}/F^2 \tag{2}$$

where T is the air-water interface tension $T \approx 0.073$ N/m; and ρ denotes water density $\rho = 1000$ kg/m^3. Then, the linear free-surface condition is:

$$\phi_{xx} + \phi_z + \sigma^2 \phi_{zzz} = 0 \quad \text{on} \quad z = 0 \tag{3}$$

By making Fourier transform to the free-surface condition, we can obtain the dispersion relation:

$$D = \alpha^2 - \sqrt{\alpha^2 + \beta^2} - \sigma^2 \left(\alpha^2 + \beta^2\right)^{3/2} = k^2 \cos^2\theta - k - \sigma^2 k^3 \tag{4}$$

with $(\alpha, \beta) = k(\cos\theta, \sin\theta)$. Dispersion curves defined by $D = 0$ are symmetrical with respect to $\alpha = 0$ and $\beta = 0$. In the quadrant $\alpha \geq 0$ and $\beta \geq 0$, dispersion curves are defined by:

$$\begin{cases} k_G = 2/(\cos^2\theta + \sqrt{\cos^4\theta - 4\sigma^2}) & \text{as} \quad k \leq k_\sigma \\ k_T = (\cos^2\theta + \sqrt{\cos^4\theta - 4\sigma^2})/(2\sigma^2) & \text{as} \quad k \geq k_\sigma \end{cases} \tag{5}$$

with $k_\sigma = 1/\sigma$. In (5), k_G denotes the wavenumber of gravity-dominant waves, and k_T represents the wavenumber of waves where the capillarity plays a dominant role following [2]. The dispersion curve is closed and confined in the region:

$$0 \leq |\theta| \leq \theta_\sigma \quad \text{with} \quad \theta_\sigma = \arctan\sqrt{(1 - 2\sigma)/(2\sigma)} \tag{6}$$

with $\sigma \leq 0.5$. When $\sigma > 0.5$, θ_σ does not exist, nor does the dispersion curve. At $\sigma = 0.5$ with the corresponding speed $c_{\min} \approx 0.2313$ m/s, the dispersion curve reduces to an isolated point at $(\alpha, \beta) = (2, 0)$ and $\theta_\sigma = 0$ according to (6) which means that all waves disappear. Therefore, waves cannot be generated as the travelling speed c is less than the critical speed $c_{\min}$.

3. FAR-FIELD WAVES AND RAY-ANGLES

Far-field waves are determined by stationary points of the phase function $\varphi = x\alpha + y\beta$, and the stationary-phase relation is:

$$\varphi' = x\alpha' + y\beta' = 0 \quad \text{with} \quad \alpha' = \mathrm{d}\alpha/\mathrm{d}k \quad \text{and} \quad \beta' = \mathrm{d}\beta/\mathrm{d}k \tag{7}$$

which gives rise to $(-x, y) \propto (\beta', \alpha')$. Following [6], far-field waves are associated with the dispersion curve $D = 0$. Differentiating $D = 0$ with respect to k yields:

$$D' = D_\alpha \alpha' + D_\beta \beta' = 0 \tag{8a}$$

$$D'' = D_\alpha \alpha'' + D_{\alpha\alpha}(\alpha')^2 + 2D_{\alpha\beta}\alpha'\beta' + D_{\beta\beta}(\beta')^2 + D_\beta \beta'' = 0 \tag{8b}$$

Combining (7) and (8a), we have the following formulation:

$$xD_\beta - yD_\alpha = 0 = h\|\nabla D\| \sin(\vartheta - \gamma) \quad \text{with} \quad (x, y) = h\,(\cos\gamma, \sin\gamma) \tag{9}$$

where ϑ is the angle between the unit vector normal to the dispersion curve and $\alpha-$axis:

$$(\cos\vartheta, \sin\vartheta) = (D_\alpha, D_\beta)\,/\|\nabla D\| \tag{10}$$

Formulation (9) holds only when $\vartheta = \gamma$ or $\vartheta = \gamma + \pi$. Hence, we can get the geometrical relationship between dispersion curve and the corresponding wave pattern which states that a point on the dispersion curve generates waves in the direction parallel to the normal direction of the dispersion curve. Introducing formulation (9) into the phase function $\varphi = x\alpha + y\beta$, we can obtain the crestlines along which the phase φ is constant:

$$(x_n, y_n) = \varphi_n \frac{(D_\alpha, D_\beta)}{\alpha D_\alpha + \beta D_\beta} \quad \text{with} \quad n = 1, 2, \cdots \tag{11}$$

where the sequence of phase is defined as [1]: $\varphi_n = -2n\pi \cdot \mathrm{sgn}(\alpha^2 D_\alpha + \alpha\beta D_\beta)$. The wave pattern is usually located between two cusps or asymptotes of a sector symmetrical about $x-$axis, and the angle between each cusp or asymptote and $x-$axis is determined by the inflection point along the dispersion curve requiring $\varphi'' = 0$ [4]. Introducing (8b) into $\varphi'' = 0$ gives rise to:

$$\varphi'' = 0 = \delta\sqrt{\alpha'^2 + \beta'^2}\, h\,(\alpha' \cos\gamma - \beta' \sin\gamma)\,/\sin 2\gamma \tag{12}$$

where the curvature δ is defined by

$$\delta = (2D_\alpha D_\beta D_{\alpha\beta} - D_\alpha^2 D_{\beta\beta} - D_\beta^2 D_{\alpha\alpha})/\|\nabla D\|^3 \tag{13}$$

The vanishing of φ'' occurs only at inflection points at $\delta = 0$ which is equivalent to:

$$3\sigma^6 k^6 - 6\sigma^4 k^5 + 23\sigma^4 k^4 - 12\sigma^2 k^3 + 9\sigma^2 k^2 + 2k - 3 = 0 \tag{14}$$

The value of σ located in the interval $[0.0, 0.5]$ determines the number of roots of (14). When σ is small (slightly greater than 0.0), there are two different inflection points (α_1, β_1) and (α_2, β_2) corresponding to two cusp angles γ_1 and γ_2 called as gravity cusp angle and capillary cusp angle baptized by Moisy & Rabaud [5]. With increasing σ, there is a critical value $\sigma = \sigma_{\mathrm{fan}} \approx 0.1331$ (travelling speed is $c = c_{\mathrm{fan}} \approx 0.4484$ m/s, and wavenumber is $k = k_{\mathrm{fan}} \approx 2.0764$) at which two inflection points coincide and $\gamma_1 = \gamma_2$. When σ is larger then σ_{fan}, no inflection point exists. Besides cusp angles associated with inflection points along the dispersion curve, the point $(\alpha_\sigma, \beta_\sigma)$ separating the dispersion curve into gravity-dominant and capillarity-dominant components corresponds to an asymptote angle designated as γ_σ which is expressed as:

$$\gamma_\sigma = \pi/2 - \theta_\sigma = \pi/2 - \arctan\sqrt{(1 - 2\sigma)/(2\sigma)} \tag{15}$$

The asymptote angle γ_σ separates the gravity-dominant and capillarity-dominant waves. In (15), the asymptote angle γ_σ is equal to 0 at $\sigma = 0$ which means that no capillary-dominant waves exist, and it equals to $\pi/2$ at the critical value $\sigma = 0.5$ with the corresponding speed

$c = c_{\min} \approx 0.2313$ m/s. In addition, the phase velocity $\vec{v}_p$ and group velocity $\vec{v}_g$ can also be determined by the dispersion relation and they are given by [4]:

$$\vec{v}_p = -(\alpha, \beta) f/k^2 \quad \text{and} \quad \vec{v}_g = -(\partial f/\partial\alpha, \partial f/\partial\beta) = -0.5(D_\alpha, D_\beta)/\alpha \tag{16}$$

where f denotes the circular frequency which is zero here (stationary wave pattern in the translating frame of reference), and it means that the magnitude of the phase speed is zero. However, we may determine the direction that the phase propagates by letting $f = 0+$. Therefore, the directions that the phase and energy propagate are associated with the wavenumber vector (α, β) and the vector normal to the dispersion curve (D_α, D_β), respectively.

4. RESULTS AND DISCUSSIONS

Figure 1 including 3 subfigures presents the dispersion curve along which gravity is dominant on the Fourier plane and corresponding crestlines and ray-angles of far-field waves for different values of σ. In addition, the directions that phase and energy propagate are also illustrated.

Subfigure (a) depicts the case of $\sigma = 0.04 < \sigma_{\text{fan}}$, at which there are two different inflection points along the dispersion curve corresponding to the gravity cusp angle γ_1 and capillary cusp angle γ_2 on the physical plane. The gravity-dominant dispersion curve is divided by two inflection points into three portions corresponding to three wave systems. The first bifurcation $k \leq k_1 = \sqrt{\alpha_1^2 + \beta_1^2}$ corresponds to transverse waves in the region of $0 \leq \gamma \leq \gamma_1$. The second bifurcation confined in $k_1 \leq k \leq k_2 = \sqrt{\alpha_2^2 + \beta_2^2}$ is associated with the divergent waves contained within the gravity cusp line and capillary cusp line $\gamma_2 \leq \gamma \leq \gamma_1$. The third one subjected to $k_2 \leq k \leq k_\sigma$ corresponds to the fan waves appearing between the capillary cusp and asymptote in the region of $\gamma_2 \leq \gamma \leq \gamma_\sigma$.

In subfigure (b) where $\sigma = \sigma_{\text{fan}} \approx 0.1331$, two inflection points coincide resulting in $\gamma_1 = \gamma_2$ which means that divergent waves contained in $\gamma_2 \leq \gamma \leq \gamma_1$ disappear. The dispersion curve along which gravity is dominant is divided by the coalesced inflection point into two portions corresponding to two wave systems on the free surface including: transverse waves in the region of $0 \leq \gamma \leq \gamma_1$ and fan waves contained in $\gamma_1 \leq \gamma \leq \gamma_\sigma$, which are joint together. In subfigure (c) where $\sigma = 0.16 > \sigma_{\text{fan}}$, there is no inflection point and cusp angles γ_1 and γ_2 do not exist. A remarkable feature is that transverse waves and fan waves appearing in subfigures (a) and (b) are merged to form a new wave system contained in the region of $0 \leq \gamma \leq \gamma_\sigma$, and we refer to this new wave system as "transverse-fan waves".

In Fig. 1, fan waves are found to extend to infinity. Indeed, the point on the dispersion curve corresponding to the point on the free surface at infinity is $(\alpha_\sigma, \beta_\sigma)$. Associated with this point, the wavenumber vector is tangent to the dispersion curve, and thus we have $(\alpha, \beta) \cdot (D_\alpha, D_\beta) = 0 = \alpha D_\alpha + \beta D_\beta$ which indicates that the corresponding point of crestlines on the physical plane is at infinity, according to (11). Crestlines of this wave system associated with different phases are nearly parallel and straight. For this reason, we call this wave system as "fan waves".

The foregoing study is concerned with the wave pattern generated by a point perturbation. However, practical observations of ship wakes are significantly narrower than Kelvin's angle [8] which is caused by the interference between waves created by bow and stern of a ship. To investigate the interference, two models are put forward including: a pressure patch with Gaussian distribution [3] and the 2-point wavemaker model [7] yielding laws of F^{-1} and F^{-2} at high Froude numbers, respectively. In the light of slender features of a ship, we adopt the latter one. Here, only downstream gravity-dominant waves interference is accounted for. Following [7], the constructive interference occurs at:

$$\frac{\ell \cos\theta}{F^2 L} = \frac{\lambda}{2} = \frac{\pi}{2}\left(\cos^2\theta + \sqrt{\cos^4\theta - 4\sigma^2}\right) \tag{17}$$

where ℓ denotes the effective distance between bow and stern, and one commonly used empirical value is $\ell = 0.9L$ [7]. Figure 2 demonstrates the apparent wake angle varying with the Froude

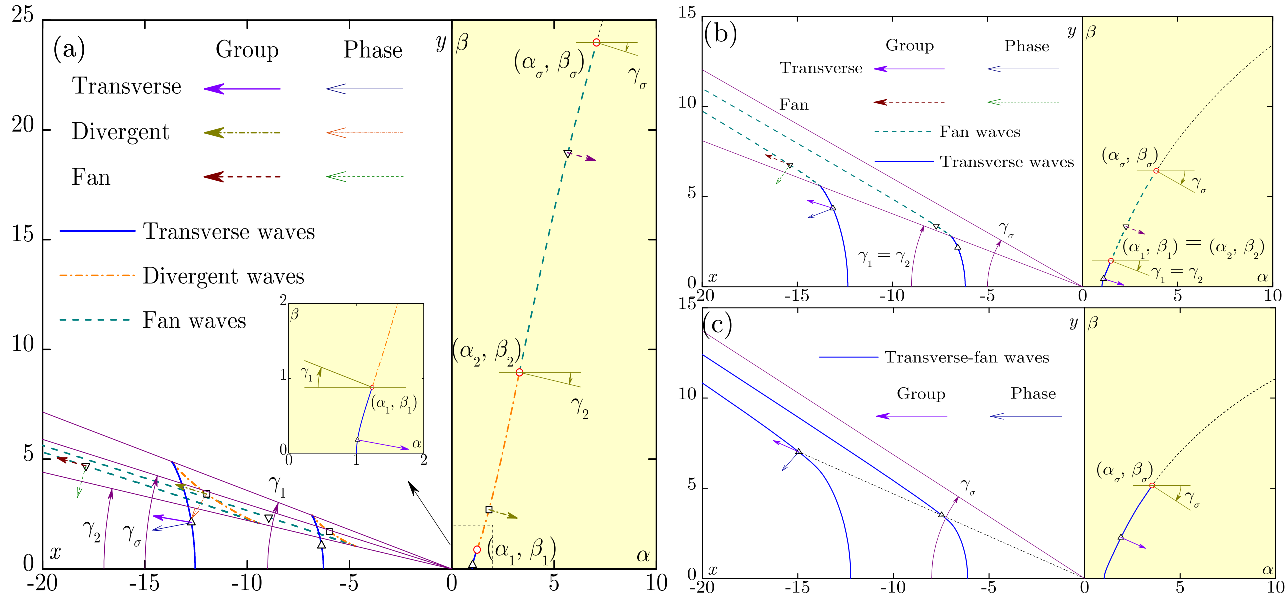

Figure 1: Gravity-dominant dispersion curve and corresponding wave crestlines as well as cusp or asymptote of capillary-gravity waves for different σ. (a): $\sigma = 0.04$; (b): $\sigma = 0.1331$; (c): $\sigma = 0.16$.

number F and comparison is made with the experimental observations by Rabaud & Moisy [8] as well as the pure-gravity solution by Noblesse et al [7]. When the Froude number is greater than 0.3, the influence of the surface tension effect on the apparent wake angle is insignificant and there is no obvious difference from the pure-gravity solution. As the Froude number is less than 0.3, the wake angle of capillary-gravity ship waves is larger than the Kelvin's angle and the surface tension effect can expound the observations that exceed the Kelvin's angle limit.

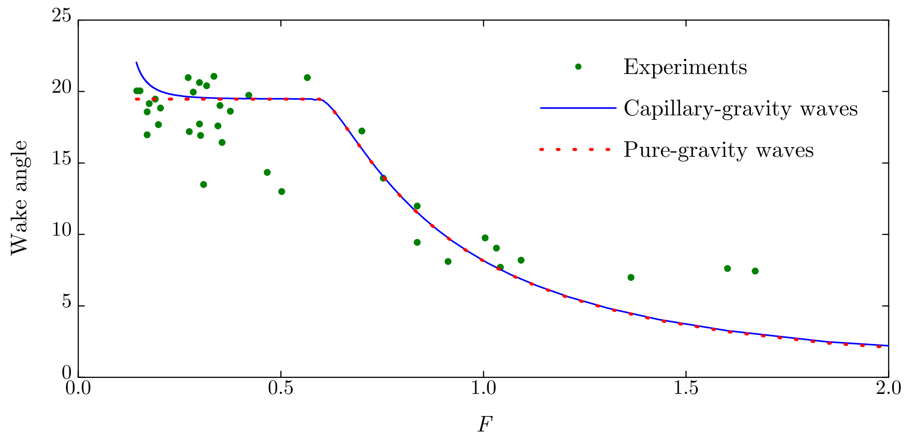

Figure 2: Wake angle varying with the Froude number. Comparison is made between theoretical predictions by the 2-point wavemaker model [7] and experimental observations [8].

REFERENCES

1 Chen XB. 2004 *Advances in Engineering Mechanics*, pp. 371-389. World Scientific Publishing.

2 Crapper GD. 1964 *Phil. Trans. R. Soc. Lond.* 282, 547-558.

3 Darmon A, Benzaquen M, Raphael E. *J. Fluid Mech.* 738, R3.

4 Lighthill J. 2001 *Waves in Fluids*. Cambridge Univ. Press.

5 Moisy F, Rabaud M. 2014 *Phys. Rev. E* 90 (2), 023009.

6 Noblesse F, Chen XB. 1995 *Ship Technol. Res.* 42, 167-185.

7 Noblesse F, He J, Zhu Y, Hong L, Zhang C, Zhu R, Yang C. 2014 *Eur. J. Mech. B-Fluids* 46, 164-171.

8 Rabaud M, Moisy F. 2013 *Phys. Rev. Lett.* 110 (21), 214503.